EDITAL DE CHAMADA PÚBLICA Nº 01/2020

Relatório final

Projeto: Geoquímica e isótopos aplicados ao estudo geoecológico das cavernas da região de Carajás

Apresentação

Durante o tempo de vigência do projeto foram coletadas amostras mensais (entre novembro de 2020 e outubro de 2021) de água de percolação (gotejamento de espeleotema), superficiais (córrego e lago) em duas cavernas (N3-23 e S11D01) num total de 60 amostras. Foram também coletadas águas de chuva no mesmo período em três locais (Escritório ICMBIO Carajás, Escritório ICMBIO Paraupebas e em Canaã dos Carajás). Nessas etapas de campo contamos com a colaboração pessoal e logística do ICMBIO. Nessas amostras foram determinados pH, condutividade, alcalinidade, cátions (K^+, Na^+, Ca^{2+}, Mg^{2+}) e ânions (Cl^-, NO_3^-, PO_4^{2-}, SO_4^{2-}) num total de 14 parâmetros medidos. Além desses parâmetros foram analisados elementos traços por ICP-MS, com concentrações significativas para os seguintes elementos As, B, Ba, Co, Cr, Cu, Fe, Mn, Ni, Rb, Se, Sr, Ti, V, Zn, Y. e abaixo do limite de detecção para os demais (Cd, Cs, Li, Sb, Sn e ETR). Além desses elementos foram determinados isótopos de O e H nas águas o que totalizou 2890 análises. Além das amostras de água, foram analisadas 13 amostras de um espeleotema em forma de estalactite (caverna N4WS 067). Nessas amostras foram analisadas a composição mineral por difração de raios-x e determinados Al_2O_3, P_2O_5, K_2O, Fe_2O_3, Ca, Na, Mg, As, Ba, Co, Cr, Cu, Mo, Ni, Pb, Rb, Se, Sr, Th, V, U, Zn e Y. Além dessas análises foram quantificados os ETR e os isótopos de Nd que devido ao baixo teor nesses elementos não tiveram um resultado satisfatório, num total de 195 elementos analisados.

Atuaram nesse trabalho:

Bolsista de IC: Juliana da Silva Araujo responsável pela coleta das amostras mensais. Colaboraram nessa etapa: 2 bolsistas de doutorado: Vitória Rodrigues Ferreira Barbosa e Rodrigo Tokuta Castro que auxiliaram no trabalho de campo e nas análises químicas;

Professores: Adriana Maria Coimbra Horbe (coordenadora do projeto), Dermeval Aparecido do Carmo, Jeremie Garnier, Patrick Seyler, Nicolas Patris e Remi Freydier responsáveis pela logística de campo, preparação das amostras para análises, análises, compilação dos resultados e preparação dos relatórios parciais e final.

Relatório final – 1a. versão do artigo

Adriana Maria Coimbra Horbe[1], Jeremie Garnier[1], Juliana da Silva Araujo[1], Vitória Rodrigues Ferreira Barbosa[1], Rodrigo Tokuta Castro[1], Nicolas Patris[3], Remi Freydier[3], Patrick Seyler[3]

1. Universidade de Brasília, Instituto de Geociências, Campus Universitário Darcy Ribeiro, 70910-900 Brasília, Distrito Federal, Brazil; 2. Laboratoire Mutualisé d'Analyse des Isotopes Stables de L'eau - HSM, Montpellier, France,

1. Introduction

Caves may be formed by several types of reactions in consequence of water dynamic, temperature and/or relative humidity, solution chemistry, pH/Eh, carbon dioxide partial pressure mediated by bones and excrements of various animals, especially bat (Onac and Forti, 2011a and b). In this environment the microorganisms, as bacterial potentiate the rocks corrosion and speleothem assemble (Onac and Forti, 2011b, Calapa et al. 2021). Although most of the caves chemical deposits are calcium carbonate, the cave environment accommodates a wide range of authigenic minerals related with geology and fluid composition. One of the most important processes inside the cave is dissolution and precipitation, that according to Eh and pH solutions form condition to precipitate a variety of carbonate, halides, oxides and hydroxides, sulfates, nitrates and phosphates (Onac and Forti, 2011b). The decaying forest-litter and guano are the main source of sulfates, nitrates and phosphates.

In Brazil there are caves formed in banded iron formations (BIF), iron ore and lateritic duricrust (Maurity and Kotschoubey, 1995, Figueira et al. 2019, Calapa et al. 2021, Parker et al. 2022, Pilo et al. 2023). Although these rocks are poor soluble, the porosity especially in the lateritic duricrust -BIF interface and the bacteria microbial Fe^{3+} reduction allowed the formation of the thousand's small caves and fissures in the Quadrilatero Ferrífero and Carajás iron ore mines. The coralloid and stalactite speleothem types are exotic sulfates and phosphates minerals: aluminite, felsőbanyaite, jarosite, spheniscidite, phosphosiderite, strengite and amorphous phosphatic material resulting from bat guano and bone accumulation and the iron and aluminum supplied by the banded iron formations (BIF), iron ore and lateritic duricrust (Figueira et al. 2019). Although, the main process and the speleothem seem to have been clarified, few is known about the effect of climatic controls on the cave surrounding environmental and the water chemistry that control rocks dissolution and mineral precipitation. The cave climatic controls that can be better highlight by $\delta^{18}O$ and δ D (Feng et al. 2014), can be determined measuring the rainwater precipitation composition relative the geochemistry on the water infiltration (Herman 2019). The vegetation and human activity impact can be detected by the geochemistry of the rainwater (Honório et al. 2017, Lachniet and Patterson 2009)

This research determined the rainwater and the cave infiltration water geochemistry, as well as the mineral and chemical composition of a remarkable long phosphatic stalactite (40 cm) in the Carajás iron mine region, northeast of Brazilian Amazonia. The aim was to investigate the prevailing physicochemical environment conditions in the cave, the speleothems formation and the interaction with the external environment.

2. Materials and Methods

The Carajás region, located in the eastern portion of the Brazilian Amazonia (Figure 1), is known for the iron, gold, copper and manganese mines. In the iron mine there are more than 2000 caves developed from the dissolution of banded iron formations (BIF) of Grão Pará Group and Itacaiunas Supergroup, iron ore and/or of ferruginous and aluminous lateritic duricrusts (Maurity and Kotschoubey, 1995; Albuquerque et al., 2018, Figueira et al. 2019). The caves range between 3 and 200 m long and 2 to 10 m tall, developed on the top of mountain slopes ridges, close to and in the BIF/lateritic duricrust interface.

The Carajás region, in the south of the Equator in eastern Amazonia (Figure 1), has an average temperature between 19° in the wet season and 32 °C in the dry season, and the precipitation average is between 1650 and 2500 mm year^{-1}. Seasonality is marked by rainfall, with the rainy season from December to May and the dry season from June to November. Paraupebas and Canaã have higher average temperatures between 21 to 35°C in consequence of their lower topographic altitude (less than 300 m and Carajás almost 700 m).

For this study, were sampled a remarkable and unusual long phosphatic stalactite speleothem (cave N4WS 067) to know better the mineral and chemical speleothem zonation. It has 42 cm long from where 13 subsamples were collected in the laboratory with a small drill equipment following the color changes. This cave is closer to the iron exploration mine (Figure 1), in the slope of the plateau and has a room of at least 17 m long and 101 m^2 with a beat's colony, however there is no regular infiltration water. According to mine classification the cave has medium species richness and low diversity of organic substrates.

To determine the cave environmental conditions and local influences, infiltration waters in two small caves were sampled (N3-23 and S11D-01). The caves close to the iron exploration mine (Figure 1), have small rooms of up to 5 m long, regular infiltration water which indicate higher water table, but there are few speleothems. The infiltration water in the caves runs into creeks and in N3-23 cave to a small lake (Violão lake). The infiltration as dripping water, the creek, as well as the lake waters were sampled.

To complement the study, the infiltration waters were compared to the rainwater composition to have information about the environment conditions in time and space of this important region of Amazonia. The rainwater of Carajás was sampled in the Carajás village mine that represent the big environment of the caves, Paraupebas that is the biggest and nearest city of Carajás with almost 214,000 hab, and Canaã, 49 km far from Carajás, that is a smaller city with almost 36,000 hab (Figure 1). The samples were collected monthly from December 21 to July 22. This period covers the dry season (May to November) and the wet season (December to April) in the Amazon region. The stalactite mineral composition was carried by X-ray diffractometer (Rigaku-Ultimate IV, with Cu tube) and the chemical composition quantified Al_2O_3, P_2O_5, K_2O, Fe_2O_3, Ca, Na, Mg, As, Ba, Co, Cr, Cu, Mo, Ni, Pb, Rb, Se, Sr, Th, V, U, Zn, Y and REE in 13 samples. The grounded stalactite samples were weighed in a Savillex® PFA vials and digested on a hot plate using a multiple-step acid procedure with HF, HNO_3 and HCl (double-distilled ultrapure acids (Merck, Germany) at sub-boiling temperatures in Teflon stills). The final solid was redissolved with 10 mL of diluted HNO_3 and centrifuged to further analysis by ICP-OES (5100 Agilent, at Geochemistry laboratory of the University of Brasilia) and ICP-MS (ICAP Q-Thermo F. Scientific, At HSM laboratory, France).

The dripping, creek and lake water sampling were done manually. For the rainwater samples it was used a manually collector (funnel-type) at approximately 1.5 m above the ground. The collectors placed in open area, were permanently fixed to the ground and removed only in the end of the experiments accumulating all coarse particles from the ambient air (wet deposition). To avoid contamination, the funnel and the bottles used for sampling and storing the water samples were cleaned with HNO_3 (5%) for 24 h. The bottles were then rinsed three times with Milli-Q water (0.2 μS cm−1). After collection, pH and conductivity of water sample were determined by WTW multiparameter and all water samples were filtered through a 0.45 μm Millipore® membrane filter. Two water aliquots samples were used to measure anions (Cl^-, NO_3^-, PO_4^{2-}, SO_4^{2-}) and the O and H isotopes, and a third aliquot was acidified with bi-distilled HNO_3 to measure major cations (K^+, Na^+, Ca^{2+}, Mg^{2+} and trace elements As, B, Ba, Cd, Co, Cr, Cs, Cu, Fe, Li, Mn, Ni, Rb, Sb, Se, Sn, Sr, Ti, V, Zn, Y, Li, Sb, Sn and REE). The anions were determined by ion chromatography (881 Compact IC pro, Metrohm), the cation by ICP-OES (5100, Agilent) and SiO_2 by colorimetry at Universidade de Brasília and the trace elements by ICP-MS (ICAP Q-Thermo F. Scientific, At HSM laboratory, France). The H^+ concentration was calculated from the pH.

For isotopic analysis, all water samples were sealed in 30 ml high-density polyethylene bottles and were analyzed at the HSM – LAboratoire Mutualisé d'Analyse des isotopes stables de l'eau, where 18O/16O and 2H/1H ratios were measured using standard methods. Water-stable isotopes were measured with an Isoprime® mass spectrometer on the LAMA platform of HydroSciences Montpellier, with an overall precision of ±0.6‰. Water isotopic compositions are reported as $\delta^{18}O$ and $\delta^{2}H$ on the V-SMOW scale.

The water concentrations of the elements were standardized by rainwater volume as volume-weighted mean concentrations (VWM) according to the formula: CVWM=[(CxxVx)/ΣVx] where Cx is the element concentration and Vx the rainwater volume of the collected rain event x. Since there is only the Carajás meteorological station data in the region, all the water samples were standardized by the Carajás rainwater volume amount.

For quality control, analytical blanks were determined according to the recommendation of Rauret et al. (2000), i.e., resulting in values lower than the L.D. of analysis. For Quality Assurance (QA)/Quality Control (QC), the following certified reference materials were used: BHVO-2 for total concentration after digestion; NRC (SLRS-5) and Mississipi-03 (CRM Environment Canada) for water analysis. The accuracy of the standard samples averaged within ± 5% of certified values. The relative standard deviations of the replicates ranged from 90% to 110% (RSD).

3 Results

3.1 The mineral and chemical composition of the speleothem

The stalactite with almost 0.50 m long is zoned, it is composed of green leucophosphite-spheniscidite-strengite near the cave roof, rose phosphosiderite-sterngite in the intermediary part and green leucophosphite-spheniscidite in the extremity with transition changes among these zones (Figure 2). The minerals are hydrated iron phosphate identified by their XRD reflections: strengite in 3.1140, 4.3830, 5.5090 Cu Å with orthorhombic structure, spheniscidite in 6.7900, 5.9900, 7.6200 Cu Å with monoclinic structure; phosphosiderite in 4.6890, 2.7870, 4.3630 Cu Å with monoclinic structure and leucophosphite in 5.9700, 6.7700, 6.1200 Cu Å with monoclinic structure. All of them have a very close chemical composition although spheniscidite contain Al and leucophosphite NH_4.

The chemical composition indicates the iron phosphate assemble has slight high Fe_2O_3 relative P_2O_5 and low K_2O and Mg content in the middle of the stalactite (L16 to L29, Table 1, Figure 3). This low K_2O and Mg control the formation of the green phosphosiderite relative rose leucophosphite-spheniscidite zonation (Figure 3). Ba, Rb and Sr follow the K_2O while the other trace elements do not show correlation among them and with the mineral zonation. However, although relative the UCC, BIF and the lateritic duricrust (Figure 4 A to C respectively) most stalactite samples are depleted in the trace elements especially relative to UCC, the samples with higher K2O and Mg are slight enriched in Rb relative the BIF and LCD. There is also a slight enrichment in all samples in Pb, Th and Zn relative the BIF. Zn is the single element slight enriched relative the UCC, BIF and the lateritic duricrust.

3.2 Chemical infiltration water composition

The water chemical composition report as volume-weighted mean concentrations, reveals diluted and acid as indicate the high H^+ contents, especially in the N3-23 dripping and lake waters, and anions deficient relative the cations contents (Table 2, figure 5). The bicarbonates concentrations are close to the detection limit of the titration method (detection limit was 0.2 µmol L^{-1}, using the Gran method with a 10 ml sample volume) were do not report.

Although the creek water of N3-23 is the most homogeneous (Figure 5), the cations prevail over the anions in consequence of the acidity that control the H^+ (Table 2). However, while the cations are higher in the dry season in the dripping and in the creek water of N3-23 they are higher in the wet season in the dripping and creek water of S11D01. The anions follow the cation content, except in the dripping water of N3-23 where they are more concentrated in the wet season (Table 2). Among the cations, H+ is the more concentrated, it is flowed by Ca in the dripping, Mg and Na in the creek and Ca and Na in the lake water of N3-23. The waters of S11D01 are more diluted, especially the dripping water, however K is more concentrated in the creek water relative the others, especially in the wet season (Figure 3).

NO_3^- is the main anion followed by SO_4^{2-} in the dripping and creek waters and by PO_4^{2-} and SO_4^2 in the lake water of N3-23, while PO_4^{2-} is the main anion in the dripping water and NO_3^- and SO_4^2 are similar in the creek water of S11D01 (Table 2, Figure 5)

SiO_2 is greater in N3-23 creek water (24.82 mg L^{-1}) and Fe in the lake and in the dripping water (10.18 and 5.82, respectively), while S11D01 show a generally low content especially in the creek water (< 3 mg L^{-1}, Table 2, figure 5).

The trace elements analyzed in few samples (Table 3), show Fe has the highest concentration followed by B, Mn and Zn in the cave's waters (Figure 6). In N3-23 the creek water has the lower concentration, while the dripping and the lake water are more similar except for Ba, Cu and Ni, more concentrated in the dripping water. The remarkable high content in Ti in the dripping water of N3-23 is most probably consequence of the amorphous brown residue found in the sampled bottle in March 22.

In S11D01 the creek water is more concentrated except for B, Co with similar concentration.

3.3 Rainwater composition

The rainwaters are less acid, more diluted with total cation and anion contents are more similar than the infiltration water (Table 2, Figure 5). H^+ is the main cation, especially in the wet season and is followed by Na in Carajás and by the remarkable high Ca content in Paraupebas and in Canaã. Cl^- is the main anion in Carajás followed by SO_4^2 and NO_3^- with similar contents, while NO_3^- is remarkably high in Paraupebas and NO_3^- and SO_4^2 in Canaã.

Boron followed by Zn and Mn are the main the trace elements. Canaã has the highest trace elements concentration (Table 3, Figure 6).

3.4 $\delta^{18}O$ and δ D composition

Concerning the stable isotopic compositions, the infiltration water are more fractionated in the January, especially in S11D01 with slight difference between the dripping and the creek water (Figure 7A and B) following the rainwater behavior (Figure 7C). There is also a lower fractionation in April in N3-23 and in March in S11D01. This less dripping isotope fractionated water in January in N3-23 and in April in S11D01, can be related to some sun warming of the roof cave rock that allow local water evaporative process.

The rainwaters have high $\delta^{18}O$ and δ D temporal variability along the study period although on average they are more fractionated in the wet season (beginning of January to April) when there is the most amount of rainwater (amount effect, Figure 7C and table 4). In general, the Carajás rainwater are more fractionated while Canaã has the less fractionated and the more variable rainwater (Figure 7C) reflecting local water evaporative process.

The d values (calculated by $d=\delta D-8\delta^{18}O$) that indicate deuterium excess, are around 11 (Table 2) that agree with those estimated by Craig (1961, d=10) for many stations around the world. Deuterium excess is typical for lower humidity conditions and for higher altitudes or short distances from the coast, and depletion is a consequence of the evaporative contribution (Dincer and Paine, 1971). The d values around 10 indicate similar evaporative contribution for the wet and dry seasons in all stations (Table 4).

The rainwater and the infiltration water ($\delta D=8.33\ \delta^{18}O+13.64$) are in the range of the global rainwater regression line ($\delta D=8\ \delta^{18}O+10$) with no difference between the wet and dry seasons (Figure 7D). However, relative to a study done three years early in the region and in the same period, the study rainwaters are slight less fractionated (up to -14.3 $\delta^{18}O$ and 104.2 δD, Medgeo 2018. Figure 7).

References

Albuquerque, A.R.L., Angelica, R.S., Goncalves, D.F., Paz, S.P.A., 2018. Phosphate speleothems in caves developed in iron ores and laterites of the Carajas Mineral Province (Brazil) and a new occurrence of spheniscidite. Int. J. Speleol. 47, 53–67.

Audra, P., De Waele, J., Bentaleb, I., Chroňákov, A., Krištůfek, V., D'Angeli2, I.M. Carbone, C., Madonia, G., Vattano, M., Scopelliti, G., Cailhol, D., Vanara, N., Temovski, M., Bigot, J-Y., Nobécourt, J-C., Galli, E., Rull, F., Sanz-Arranz, A., 2019. Guano-related phosphate-rich minerals in European caves International Journal of Speleology, 48, 75-105.

Calapa KA, Mulford MK, Rieman TD, Senko JM, Auler AS, Parker CW and Barton HA 2021. Hydrologic Alteration and Enhanced Microbial Reductive Dissolution of Fe(III) (hydr)oxides Under Flow Conditions in Fe(III)-Rich Rocks: Contribution to Cave-Forming Processes. Frontiers in Microbiol. 12:696534.

da Silva, A.C.S., Costa, M.L. 2020 Genesis of the "soft" iron ore at S11D Deposit, in Carajás, Amazon Region, Brazil. Brasilian. Journal of Geology. 50, e20180128

Feng, W., Casteel, R.C., Banner, J.L, Heinze-Fry, A., 2014. Oxygen isotope variations in rainfall, drip-water and speleothem calcite from a well-ventilated cave in Texas, USA: Assessing a new speleothem temperature proxy. Geochimica et Cosmochimica Acta 127, 233–250.

Figueira, R.L., Horbe, A.M.C., Aragon, F.F.H., Goncalves, D.F. 2019. Exotic sulphate and phosphate speleothems in caves from eastern Amazonia (Carajas, Brazil): crystallographic and chemical insights. Journal of South American Earth Sciences 90, 412-422.

Herman, J.S. 2019. Water chemistry in caves. Chapter 133, Encyclopedia of Caves (Third Edition), p. 609-614

Honório, B.A.D., Horbe A.M.C. Horbe, Seyler, P. 2010. Chemical composition of rainwater in western Amazonia — Brazil. Atmospheric Research 98, 416–425.

Lachniet, M.S., Patterson, W. P. 2009. Oxygen isotope values of precipitation and surface waters in northern Central America (Belize and Guatemala) are dominated by temperature and amount effects. Earth and Planetary Science Letters 284, 435–446.

Maurity, C., Kotschoubey, W.B., 1995. Evolucao recente da cobertura de alteração no Plato N1 – Serra dos Carajas-PA. Degradacao, pseudocarstificacao, espeleotemas. Boletim do Museu Paraense Emilio Goeldi, 7, 331–362.

McLennan, S.M. 2001. Relationships between the trace element composition of sedimentary rocks and upper continental crust. Geochemistry, Geophysics, Geosystems, 2000GC000109.

MEDGEO 2018. Relatório técnico com estudos sobre a área hídrica para a cavidade S11D_0001. Medgeo, hidrologia e meio ambiente. 121p.

Onac B.P., Forti, P. 2011a. State of the art and challenges in cave minerals studies Studia UBB Geologia, 56, 33 – 42.

Onac B.P., Forti, P. 2011b. Minerogenetic mechanisms occurring in the cave environment: an overview. International Journal of Speleology 40, 70-98.

Parker, C.W., Wolf, J.A., Auler, A.S., Hazel, Barton, A., Senko, J.M. 2013. Microbial Reducibility of Fe(III) Phases Associated with the Genesis of Iron Ore Caves in the Iron Quadrangle, Minas Gerais, Brazil. Minerals 3, 395-411; doi:10.3390/min3040395

Piló, L.B., Calux, A., Scherer, R., Bernard, E. 2023. Bats as ecosystem engineers in iron ore caves in the Carajás National Forest, Brazilian Amazonia. Plos One. https://journals.plos.org/plosone/article?id=10.1371/journal.pone.0267870.

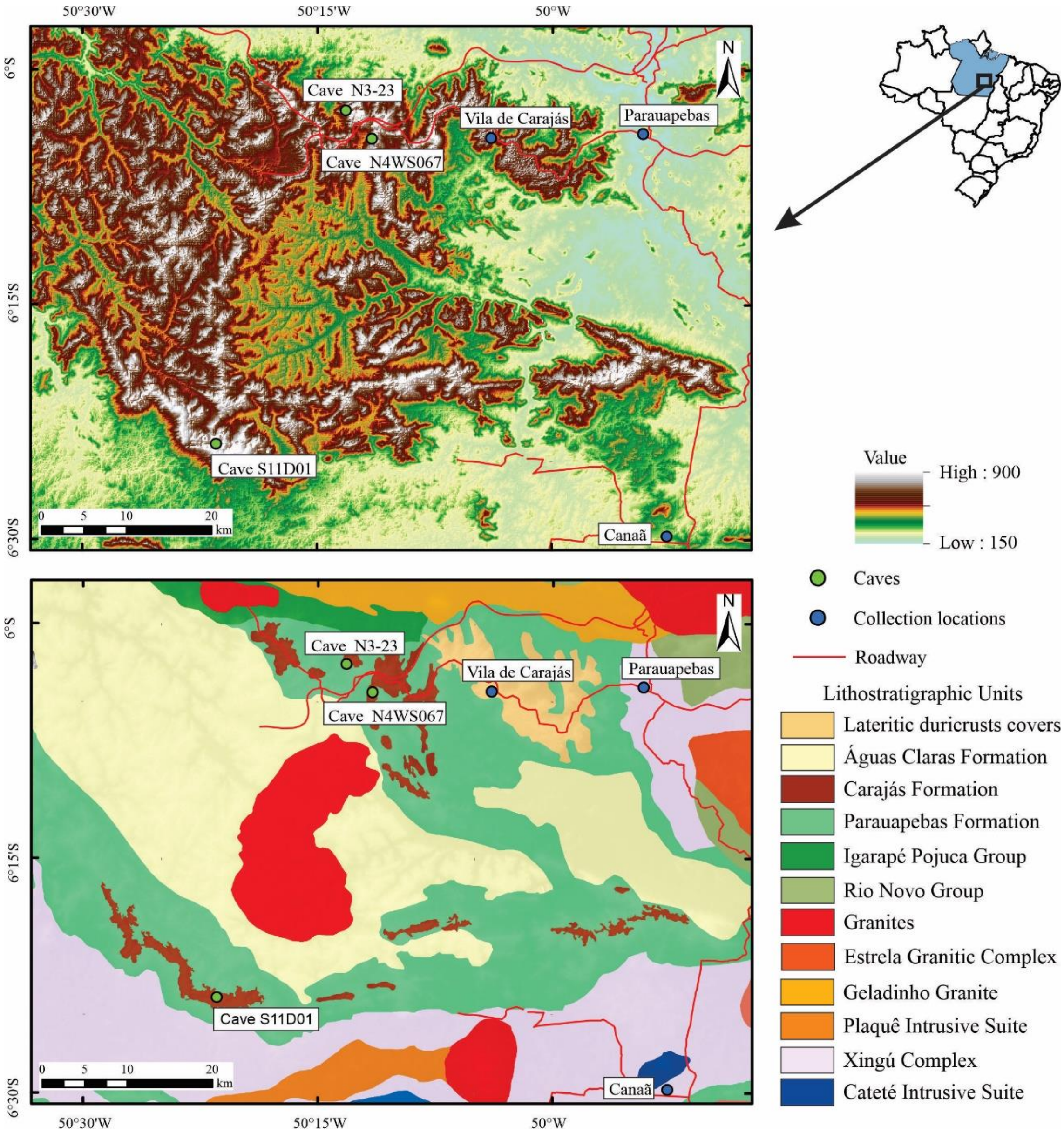

Figure 1: Geological setting with the caves and rainwater samples sites location

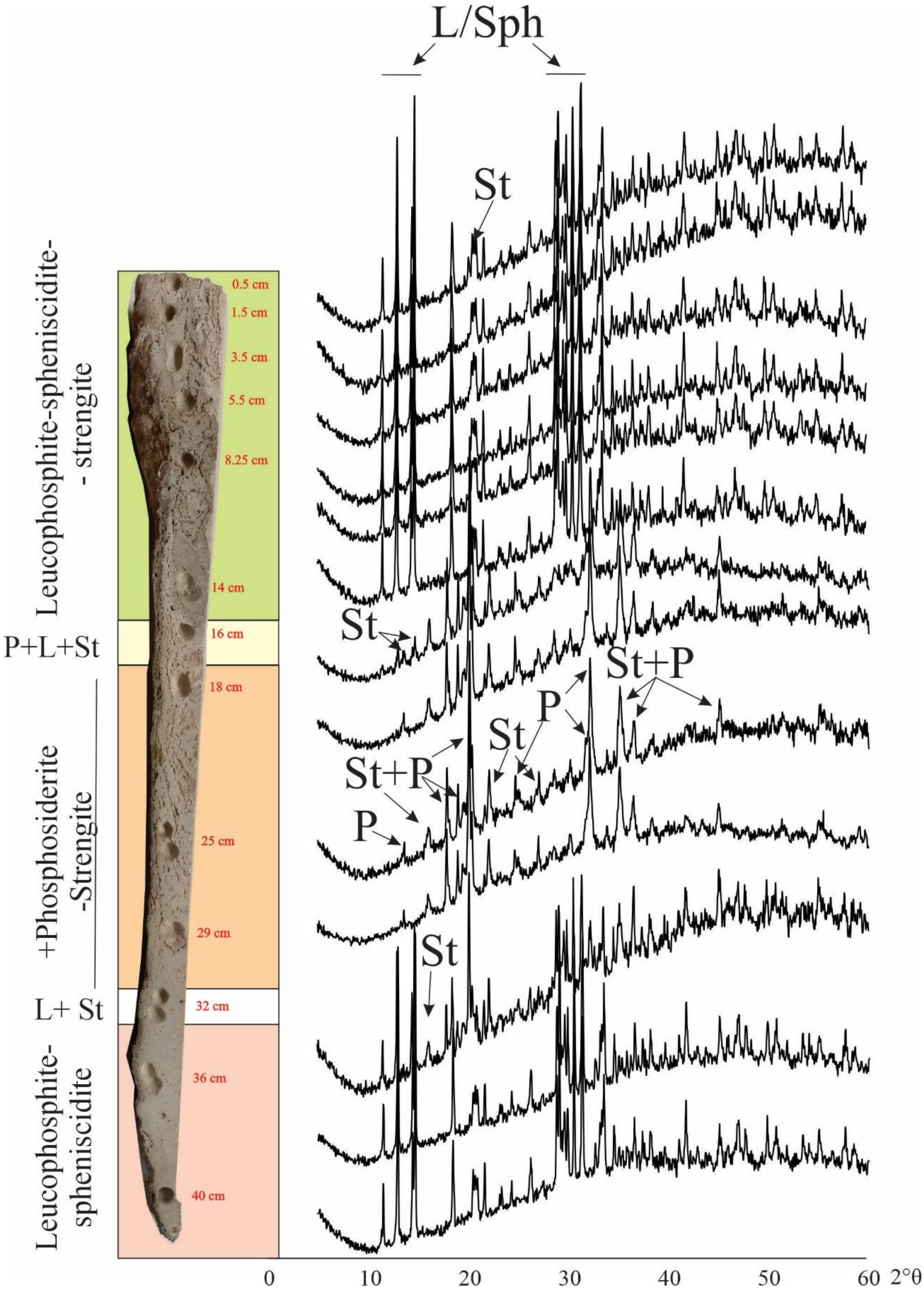

Figure 2: XRD data from the stalactite samples, P: phosphosiderite, L: leucophosphite, St strengite.

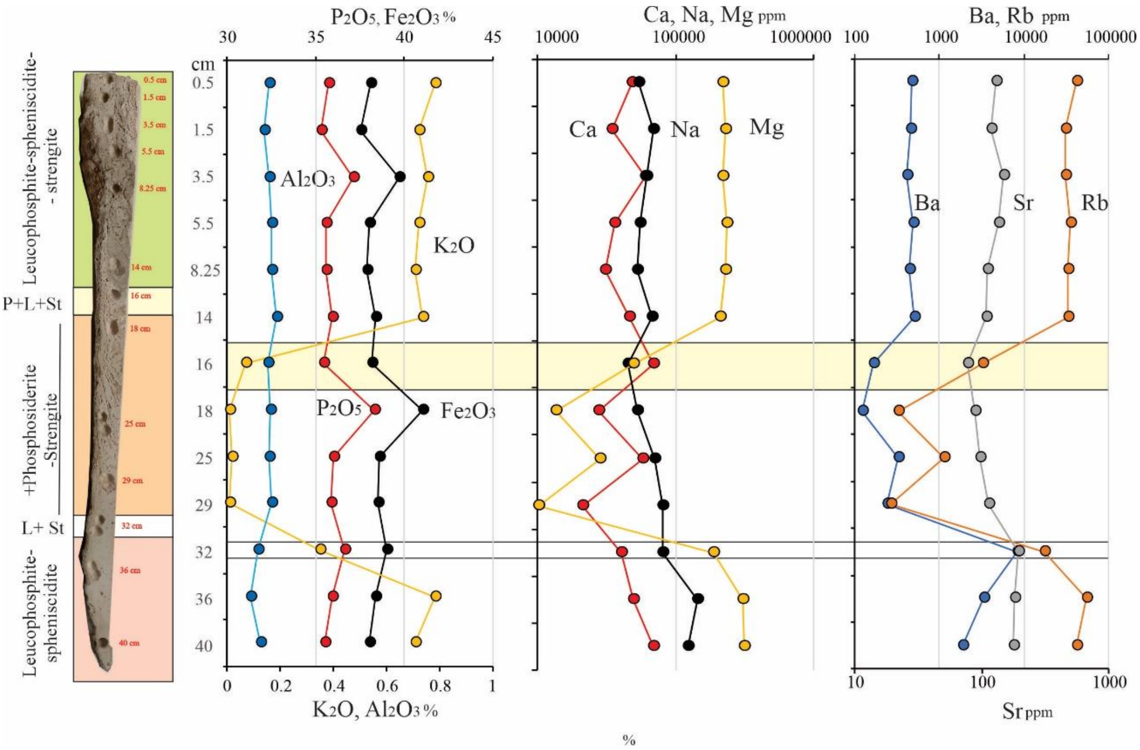

Figure 3: Chemical composition of the stalactite.

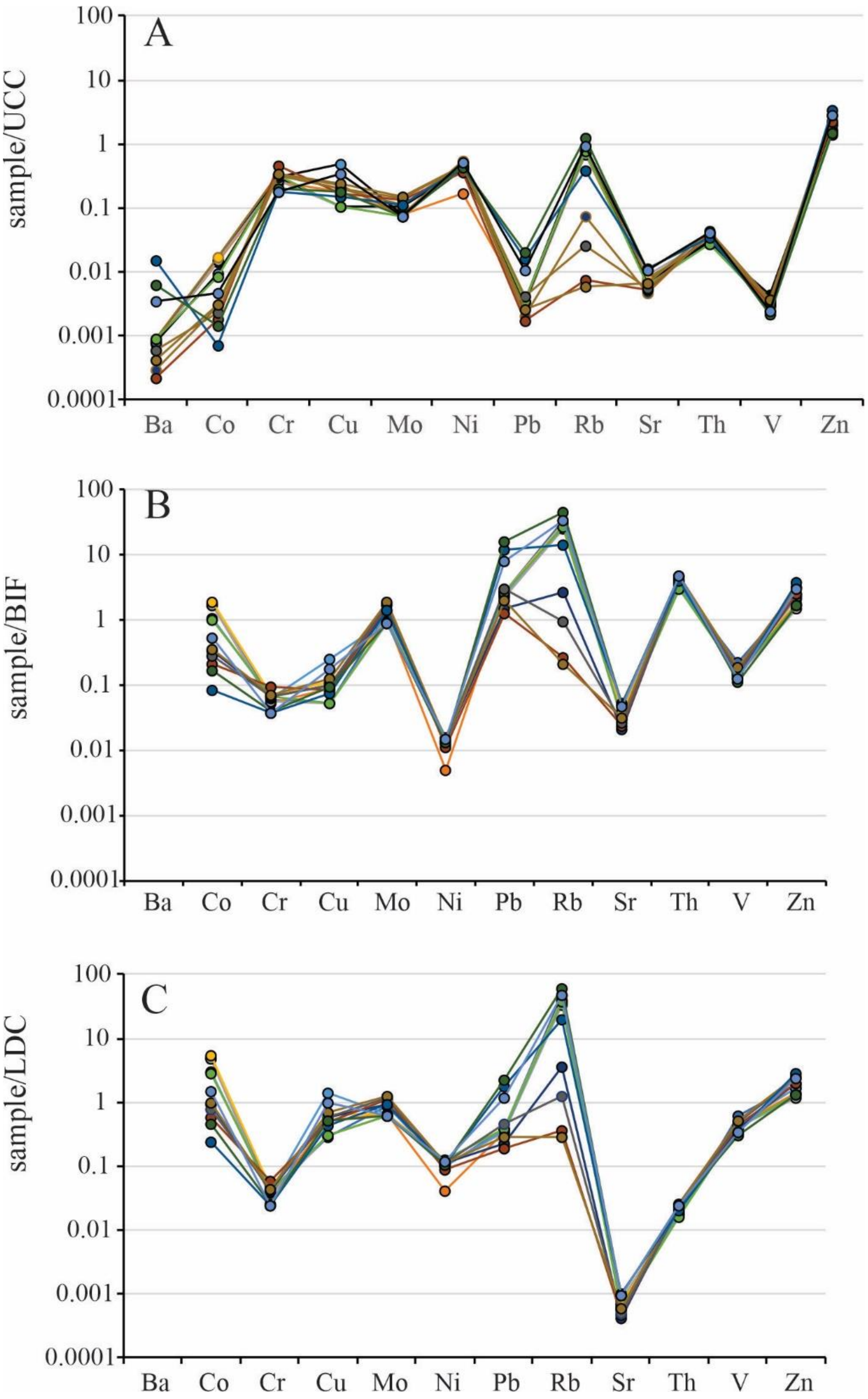

Figure 4: Trace elements fractionation relative the A: Upper continental crust (UCC) after McLennan (2001), B: banded iron formation (BIF) and C: Lateritic duricrust after Silva and Costa (2020).,

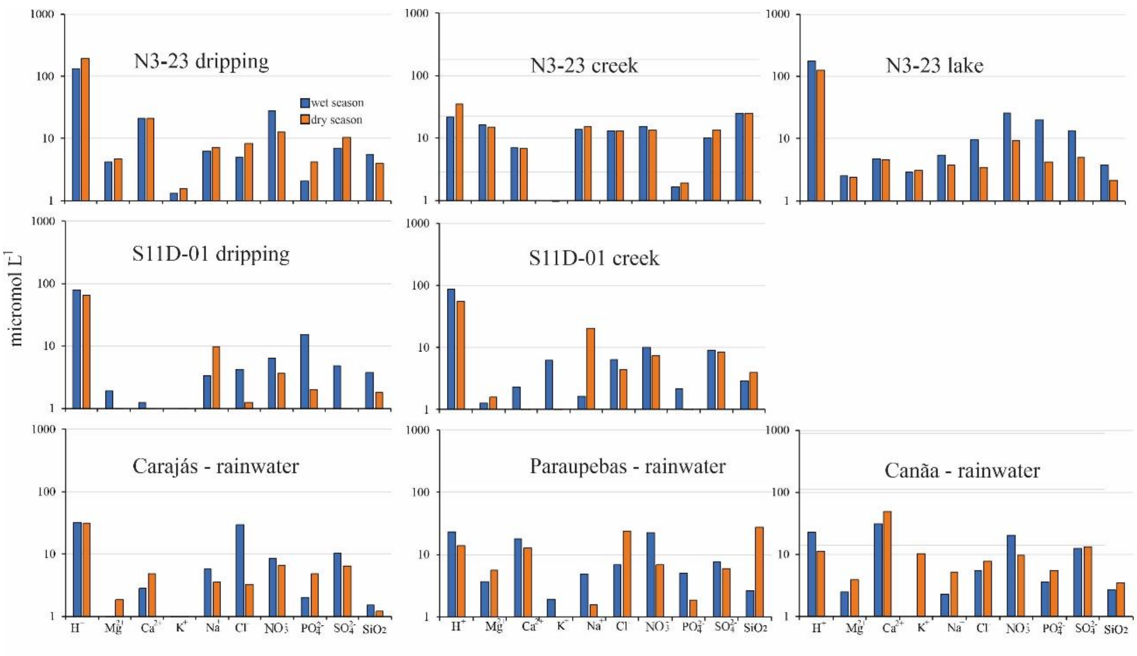

Figure 5: Main cation and anion chemical composition from the infiltration water in the caves and in the study rainwater

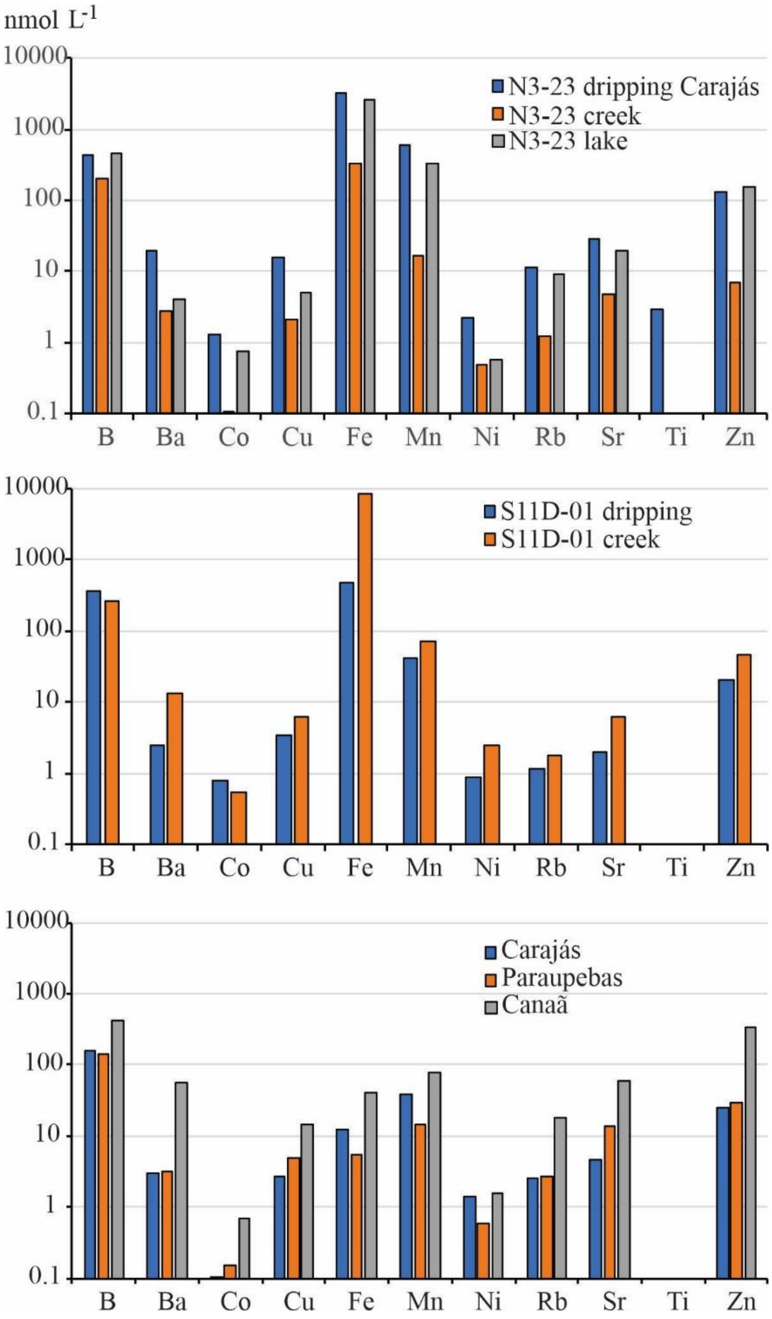

Figure 6: Trace elements chemical composition from the infiltration water in the caves and in the study rainwater

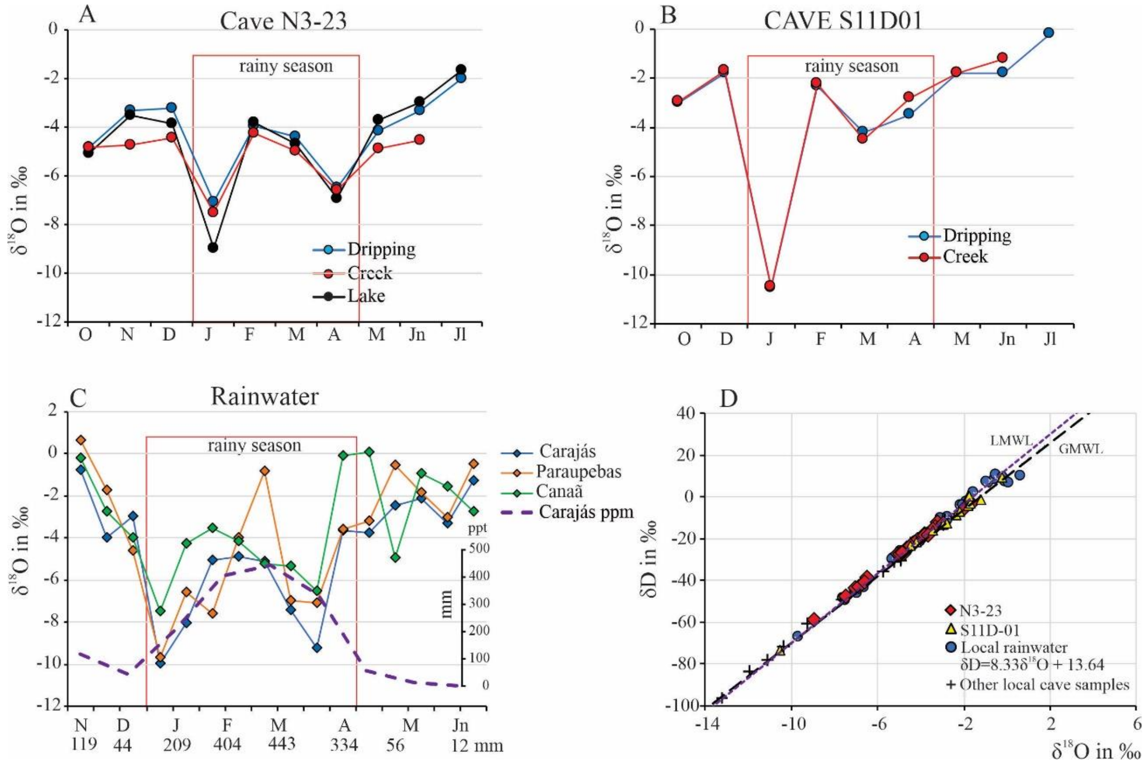

Figure 7: $\delta^{18}O$ and δ D isotopes chemical composition from the infiltration water in the caves and in the study rainwater and the local rainwater regression line

Table 1: Chemical composition of the stalactite, the oxides in %wt and the other elements in ppb. Upper continental crust (UCC) after McLennan (2001), banded iron formation (BIF) and lateritic duricrust (LDC) after Silva and Costa (2020)

Samples	**Al_2O_3**	**Fe_2O_3**	**P_2O_5**	**K_2O**	**Mg**	**Na**	**Ca**	**Ba**	**Co**	**Cr**	**Cu**	**Mo**	**Mn**	**Ni**	**Pb**	**Rb**	**Sr**	**Th**	**V**	**Zn**
L1 0.5	0.16	38.10	35.68	0.78	221730	53519	48324	468	8452	5039	8511	2587	2587	459	2142	41988	129	3326	1526	23941
L1 1.5	0.14	37.55	35.26	0.72	228150	69371	34287	447	8048	4275	14674	1985	1985	187	1885	31182	119	3917	1102	18046
L1 3.5	0.16	39.69	37.14	0.76	220802	61710	59895	409	8138	4582	8599	1815	1815	488	1818	30833	148	3703	1013	15285
L1 5.5	0.17	38.03	35.57	0.72	235009	54813	35849	484	9168	5928	18328	1977	1977	592	2132	35806	136	3461	1064	21482
L1 8.25	0.17	37.90	35.57	0.71	230587	52877	30963	437	5141	5096	41048	1952	1952	459	2027	33713	110	3397	1118	22050
L1 14	0.18	38.35	35.90	0.73	212013	67376	46093	495	4684	5424	8572	1883	1883	576	2090	33359	107	3092	1044	17021
L1 16	0.15	38.14	35.42	0.07	49559	44811	69778	162	1599	5403	17011	2814	2814	520	1207	3172	77	4485	949	25799
L1 18	0.16	41.04	38.29	0.01	13680	53331	27440	121	1006	7605	13904	3343	3343	400	1023	322	88	4315	1099	25273
L1 25	0.16	38.59	36.00	0.02	28261	70245	57765	319	1300	5605	16831	3503	3503	507	2447	1124	97	4068	1206	31660
L1 29	0.17	38.53	35.86	0.01	10268	80059	21061	237	1693	5735	20286	3700	3700	515	1571	261	113	4914	1307	31765
L1 32	0.11	38.98	36.61	0.35	189114	80236	40093	8243	401	3055	12601	2778	2778	477	9740	17266	196	3974	872	37490
L1 36	0.09	38.33	35.93	0.78	307013	142961	49957	3368	773	3364	15302	1800	1800	482	12549	55559	183	4686	765	16857
L1 40	0.12	38.02	35.53	0.71	314635	122333	69560	1887	2573	3100	29207	1801	1801	552	6433	41949	178	4663	861	30808
BIF	0.58	46.07	0.01	<0.01	1.98	<0.01	<0.01	--	4.7	83	30	2	--	37	18	1.2	3.7	1	7	10
LDC	9.67	76.14	0.78	<0.01	<0.01	<0.01	<0.01	--	1.7	130	29	3	--	4.6	5.5	0.9	191	191	2.5	13
UCC	15,19	5.00	0.16	3.37	13300	28900	30000	550	17	83	25	1.1	600	44	17	112	350	11	107	71

Table 2: Inflitration water in the study caves and rainwater composition: ppt: Carajás monthly precipitation (in mm), conductivity (C in µScm-1), major ionic composition in µmol L^{-1}, VWM volume-weight mean, VWMW in the wet season, VWMD in the drier season, Tcations: sum of the total cations and Tanions: sum of total anions.

		ppt	pH	cond	H^+	Mg^{2+}	Ca^{2+}	K^+	Na^+	Cl^-	NO_3^-	PO_4^{2-}	SO_4^{2-}	SiO_2	Total ions	Tcations	Tanions
N3-23 dripping	VWM		3.91	18.89	137.23	4.40	21.89	1.37	6.57	5.42	27.47	2.29	7.42	5.62	214.07	171.47	42.61
	VWMW		3.93	18.36	132.66	4.23	21.28	1.31	6.32	5.02	27.80	2.06	6.93	5.57	207.61	165.81	41.80
	VWMD		3.58	25.30	192.93	4.76	20.85	1.55	7.12	8.28	12.80	4.25	10.49	3.97	263.02	227.21	35.81
N3-23 creek	VWM		4.34	4.49	22.77	16.07	6.88	0.08	13.84	12.79	15.09	1.67	10.35	24.49	99.53	59.64	39.89
	VWMW		4.69	4.84	21.79	16.16	6.89	0.00	13.73	12.76	15.24	1.65	10.09	24.47	98.33	58.58	39.75
	VWMD		4.48	4.81	34.67	15.03	6.72	0.99	15.24	13.07	13.22	1.88	13.42	24.79	114.25	72.65	41.59
N3-23 lake	VWM		3.77	13.53	183.22	2.72	5.06	3.16	5.65	9.45	25.12	18.85	13.29	3.76	266.54	199.82	66.71
	VWMW		3.78	13.07	177.36	2.55	4.71	2.91	5.49	9.64	25.64	19.70	13.54	3.71	261.54	193.02	68.52
	VWMD		3.66	19.16	124.80	2.38	4.58	3.10	3.72	3.45	9.23	4.15	5.05	2.13	160.46	138.58	21.88
S11D01 dripping	VWM		4.11	4.17	77.85	1.75	1.15	0.03	4.27	3.78	5.93	13.38	4.22	3.46	112.35	85.05	27.31
	VWMW		4.11	4.10	78.91	1.91	1.25	0.00	3.35	4.21	6.32	15.28	4.81	3.75	116.04	85.42	30.61
	VWMD		4.19	5.00	64.91	0.73	0.58	0.18	9.79	1.23	3.59	2.00	0.72	1.76	83.72	76.18	7.54
S11D01 creek	VWM		4.20	3.84	83.66	1.30	2.21	5.76	3.05	6.30	9.87	2.06	9.09	3.01	123.31	95.99	27.32
	VWMW		4.19	3.75	85.98	1.28	2.32	6.21	1.64	6.45	10.07	2.19	9.13	2.93	125.27	97.43	27.84
	VWMD		4.26	4.93	55.26	1.58	0.89	0.31	20.35	4.48	7.43	0.47	8.62	3.98	99.39	78.38	21.00
Carajás	VWM	266.16	4.51	1.97	32.32	0.87	2.95	0.59	5.54	27.90	8.41	2.18	10.30	1.49	91.06	42.29	48.78
	VWMW	345.97	4.50	1.86	32.37	0.82	2.85	0.60	5.65	29.23	8.50	2.03	10.50	1.51	92.57	42.30	50.28
	VWMD	57.48	4.54	3.13	31.50	1.85	4.79	0.45	3.50	3.22	6.64	4.85	6.44	1.20	63.23	42.09	21.15
Paraupebas	VWM		4.98	4.61	21.20	3.51	16.44	1.66	4.27	7.96	19.68	4.48	7.05	4.62	86.26	47.07	39.18
	VWMW		4.89	4.64	23.18	3.66	17.99	1.89	4.85	6.87	22.42	5.07	7.68	2.58	93.61	51.58	42.04
	VWMD		4.98	9.44	13.78	5.65	12.82	0.58	1.57	24.11	6.84	1.84	5.88	27.67	73.07	34.40	38.67
Canaã	VWM		4.89	5.04	21.92	2.58	31.76	0.54	2.45	5.63	19.99	3.69	12.44	2.77	101.00	59.25	41.75
	VWMW		4.70	5.05	22.52	2.51	30.81	0.00	2.30	5.51	20.56	3.59	12.40	2.73	100.19	58.13	42.06
	VWMD		6.27	5.03	11.06	3.88	48.91	10.29	5.23	7.76	9.74	5.50	13.12	3.53	115.50	79.37	36.13

Table 3: Infiltration and rainwater trace elements in nanomol L^{-1}, ppt: monthly precipitation amount. As, Cd, Cs, Cr, Li, Sb, Se, Sn V, Y, REE > LD

Samples	ppt	B	Ba	Co	Cu	Fe	Mn	Ni	Rb	Sr	Ti	Zn
N3-23 dripping March	443.13	355	10.5	0.99	12.0	7239	552	2.0	3.1	29.3	6.64	60
N3-23 dripping October	570.16	483	27.2	1.58	18.0	165	619	2.4	18.2	28.8	<DL	186
VWM		**427**	**19.9**	**1.3**	**15.4**	**3258**	**590**	**2.2**	**11.6**	**29.0**	**2.9**	**131**
N3-23 creek June	12	269	21.9	0.47	9.4	847	131	3.4	8.3	24.4	<DL	29
N3-23 creek October	570.16	199	2.4	0.09	2.0	315	14	0.4	1.1	4.4	<DL	7
VWM		201	2.8	0.1	2.1	326	16	0.5	1.2	4.8	<DL	7
N3-23 lake January	244.09	290	5.7	0.90	4.8	8369	133	1.0	0.4	4.8	<DL	19
N3-23 lake February	570.16	547	3.3	0.70	5.1	221	419	0.4	12.5	26.1	<DL	213
N3-23 lake June	12	412	7.1	1.21	10.1	2379	458	1.1	11.1	23.7	<DL	223
VWM		469	4.0	0.8	5.1	2659	335	0.6	8.9	19.7	<DL	156
S11D01-Dripping March	443.13	266	5.2	1.40	4.1	1041	95	2.0	1.0	4.5	<DL	42
S11D01-Dripping February	570.16	431	0.2	0.34	2.8	50	2	<DL	1.2	0.2	<DL	3
S11D01-Dripping June	12	298	2.6	0.29	1.2	905	8	0.8	0.3	0.6	<DL	15
VWM		358	2.4	0.8	3.4	488	42	0.9	1.1	2.0	<DL	20
S11D01-Creek March	443.13	250	14.4	0.55	5.7	9624	79	2.4	1.9	6.5	<DL	42
S11D01-Creek January	44.3	295	4.7	0.51	13.0	793	17	2.6	0.4	2.1	<DL	86
S11D01-Creek June	12	345	2.4	0.37	2.3	877	30	0.5	0.7	2.3	<DL	19
VWM		257	13.2	0.5	6.2	8630	72	2.4	1.8	6.0	<DL	45
Carajás January	244.09	85	1.8	0.04	4.8	<DL	5	1.4	<DL	0.9	<DL	33
Carajás June	12	268	11.4	0.02	4.9	<DL	1	2.0	1.6	10.6	<DL	28
Carajás Outubro	570.16	187	3.3	0.13	1.8	18	53	<DL	3.7	6.1	<DL	21
VWM		**158**	**2.99**	**0.10**	**2.70**	**12**	**38**	**1.42**	**2.56**	**4.62**	**<DL**	**24**
Paraupebas January	244.09	67	5.6	0.38	5.5	19	28	0.9	0.3	7.3	<DL	37
Paraupebas June	12	435	22.5	0.17	7.4	<DL	8	3.2	3.9	22.3	<DL	57
Paraupebas Outubro	570.16	173	1.7	0.06	4.6	<DL	9	0.4	3.7	16.8	<DL	26
VWM		**145**	**3.2**	**0.2**	**4.9**	**6**	**15**	**0.6**	**2.7**	**14.1**	**<DL**	**30**
Canaã JMarch	443.13	191	56.5	0.41	6.7	44	21	1.0	8.0	7.1	<DL	184
Canaã June	12	300	159.5	1.64	8.0	19	79	4.9	4.4	34.0	<DL	8810
Canaã Outubro	570.16	616	55.9	0.90	20.5	40	126	1.9	26.8	100.3	<DL	271
VWM		**429**	**57.4**	**0.7**	**14.4**	**42**	**80**	**1.6**	**18.4**	**59.2**	**<DL**	**334**

Table 4: Stable isotopic (‰) of infiltration water in the study two caves and of rainwater composition.

	$\delta^{18}O$			**δD**			**Mean during wet season**			**Mean during dry season**		
	Mean	Max.	Min.	Mean	Max.	Min.	$\delta^{18}O$	δD	d	$\delta^{18}O$	δD	d
Rain Carajás	-4.26	-0.79	-9.95	-23.78	5.92	-67.87	-6.66	-41.28	11.98	-2.57	-6.62	13.96
Rain Paraupebas	-3.82	0.62	-9.65	-19.56	10.52	-67.29	-5.78	-35.45	10.81	-1.86	-3.67	11.24
Rain Canaã	-3.35	0.08	-7.46	-15.47	8.99	-49.64	-4.57	-25.45	11.14	-2.13	-5.50	11.55
N3-23 dripping	-4.26	-1.99	-7.04	-21.78	-5.49	-43.86	-5.46	-31.06	12.62	-3.46	-15.59	12.12
N3-23 creek	-5.17	-4.24	-7.47	-29.14	-21.99	-47.47	-5.81	-34.36	12.12	-4.66	-24.95	10.28
N3-23 lake	-4.50	-1.64	-8.95	-23.94	-3.11	-59.03	-6.08	-36.23	12.41	-3.44	-15.74	11.78
S11D01 dripping	-3.25	-0.21	-10.52	-14.80	9.10	-73.53	-5.14	-30.08	11.04	-1.73	-2.58	11.27
S11D01 creek	-3.46	-1.23	-10.50	-16.71	0.47	-73.33	-5.00	-29.05	10.93	-1.91	-4.36	10.94